Fine-tuning the optical properties of Fluorescent Ag-DNA and their application as fluorescence quenchers

THESIS
submitted in partial fulfillment of the
requirements for the degree of
Master of Science
in
PHYSICS

Donny de Bruin

Leiden, October 23rd 2018

Supervisor: Dirk Bouwmeester

Contents

Chapter 1 - Fine-tuning the optical properties of fluorescent Ag-DNA complexes

DNA-stabilized fluorescent silver clusters (Ag-DNAs) are an interesting new kind of fluorophore, allowing a tunable fluorescence wavelength through the design of the stabilizing DNA strand. However, the optical properties of fluorescent species stabilized by varying strand sequences are difficult to predict. We now report on the fine-tuning of the fluorescence wavelengths of one type of Ag-DNA through specific changes to its DNA host. When using hairpin-shaped DNA structures to stabilize the silver cluster, the emission wavelength can be fine-tuned within a 12nm spectral range by changing the length and sequence of the double stranded part of the native hairpin. Simultaneous changes in the excitation spectra point towards a change in the environment of the cluster within its DNA encapsulation. Varying the temperature shows that the optical properties of the system can be altered dynamically. These results constitute a significant step towards these fluorophores fulfilling their promise of tailor-made production of fluorescent emitters.

Introduction

Positioned on the boundary between the molecule and nanoparticle regimes, few-atom noble metal clusters of the order of 10 atoms in size have been the topic of significant research. Silver nanoclusters in particular show promise due to the strong fluorescence they exhibit, with a notable dependency on the size and shape of the cluster[1].

Due to this strong dependency, enabling the formation of a specific silver cluster with a specific resonance through choice of the stabilizing ligand is a tempting proposition. Additionally, due to the small size of the cluster, the chosen ligand will constitute a large contribution to its direct environment because it will be in close proximity to a large portion of its atoms. There can be significant effects on the optical properties of noble metal clusters as a result[2,3].

Design of DNA oligonucleotides has been established as a reliable way of producing fluorescent complexes consisting of a few-atom silver cluster within a short single stranded DNA encapsulation. These DNA-encapsulated silver clusters (Ag-DNAs) have been proven to be a novel way of designing a range of new fluorophores, through variation of DNA length and sequence [4–6]. Ag-DNAs have been shown to exhibit fluorescence activity with quantum yields up to 64%[7], and the silver cluster allows for a significantly larger photo stability than organic dye counterparts[8]. Finally, because the emission mechanism has been indicated to be plasmonic in nature[9], the potential for fluorescence quenching and enhancement of other fluorophores could make Ag-DNAs an attractive option in wide-ranging experiments.

The optical properties of Ag-DNAs are largely determined by the number of atoms which form the cluster, leading to several distinct species of fluorescent emitter with emissions ranging from 500nm to

800nm [10]. Smaller variations within the emission spectra are expected to be mainly dependent on the exact configuration of the Ag-DNA construct. Recent results have indicated that a DNA-silver interaction may contribute to the excitation of the fluorophore in particular[11].Thus, manipulating the configuration of structure through design of the hosting DNA strand may allow tuning of the resonance wavelengths with very high resolution.

By designing a DNA oligonucleotide to be partially self-complimentary, hairpin-shaped structures can be produced, consisting of a double-stranded 'stem' and a single stranded loop. These types of structures have been shown to allow fluorescent silver cluster formation with a poly-C single stranded loop as its primary ligand [12,13]. For some of these emitters, the double-stranded part of the ligand structure has been indicated to be relatively uninvolved with the silver cluster by measurements on their electrophoretic mobility and diffusivity[14]. In this paper, we use the native secondary structure of the DNA strand that stabilizes this particular Ag-DNA to tune its optical properties through the changing DNA environment. Step-by-step alterations to the DNA sequence lead to a tunable behavior of the optical properties of the fluorophore distribution that forms.

Materials and methods

Ag-DNA synthesis was performed under identical conditions for all used oligomers. The DNA strands (Integrated DNA Technologies) were mixed with $AgNO_3$ (99.9999%, Sigma Aldritch), in an ammonium acetate buffer (99.999%, Sigma Aldritch). The solutions were kept at 4^{o}Cfor 30 minutes, after which a freshly prepared solution of the reducing agent $NaBH_4$ is added. Final concentrations were 50 µM DNA, 350 µM$AgNO_3$, 100 µM $NaBH_4$, and 20 mM ammonium acetate. Afterwards, the solutions were left to become maximally fluorescent for 10 hours at 4 °C before use. Measurements were performed on the samples in solution in a quartz cuvette, using a Cary Eclipse fluorimeter (Varian). The temperature of the samples was controlled using a water-cooled Peltier element and controller.

The '9C'-hairpin was chosen as a DNA host as it is known to produce a significant yield of fluorescent emitters in the visible range[13]and due to its relatively well-defined DNA structure[14].

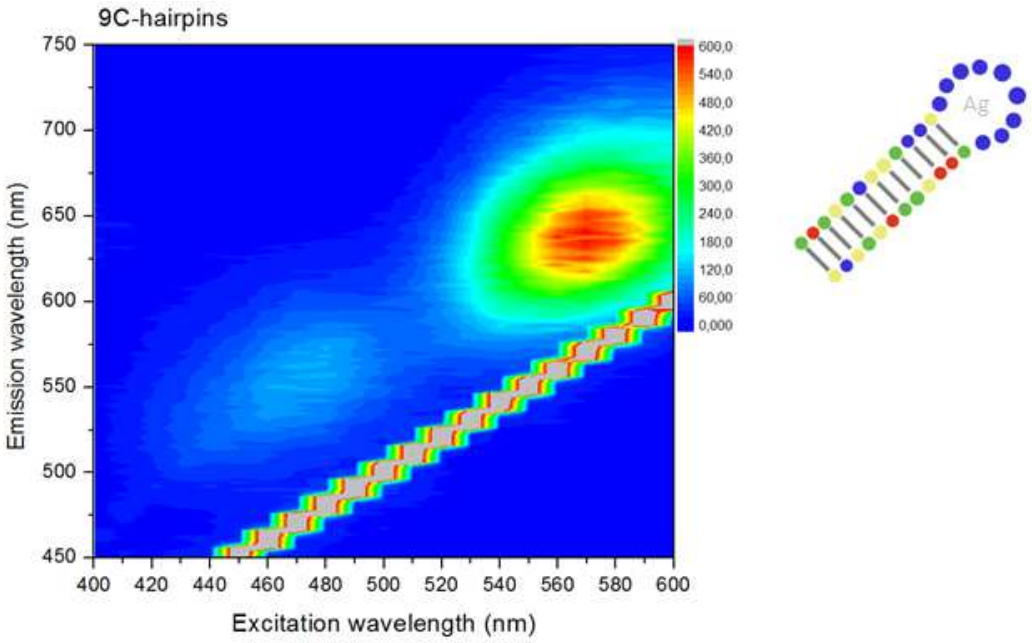

Figure 1: Fluorimetry results of ensembles of Ag-DNA formed on a 9C-hairpin DNA host performed in solution at room temperature. Excitation and emission wavelengths are plotted along the horizontal and vertical axes respectively. The emission intensity is shown in the color. The grey peaks for equal excitation and emission wavelengths are caused by scattering of the excitation light.

Figure 1 shows the fluorescence behavior of the Ag-DNAs which are formed on the chosen '9C' DNA-hairpins. The DNA strand comprises a length of nine cytosine bases with complimentary strands on either end. As a result, the strand can be expected to fold into a hairpin structure whereby only the 9C-loop remains single stranded.

These are known to produce two dominant types of fluorescent emitter, with excitation maxima around 470nm and 570nm, corresponding to two different sizes of silver cluster[13]. The green emitter with a lower resonance wavelength has been shown to be erratic with regard to the properties of the stem of the DNA hairpin, and has been determined to be likely to be formed on a disturbed DNA hairpin structure [14]. The focus of this study is on the red emitter which is centered on a 570nm excitation. These emitters have been determined to have a significantly lower diffusion rate, implying a larger hydrodynamic radius compared to the other emitters that form. It is therefore likely that these Ag-DNA complexes have a more clear distinction between the silver cluster within its encapsulation, and a secondary structure formed out of the native double stranded part. If this is the case, it should be possible to manipulate the properties of the stem without disturbing the formation of the cluster within the loop.

The double stranded stem was varied using a base pair-by-base pair method, i.e., through addition of complimentary bases to the 3' and 5' ends of the DNA strand. This process has the effect of elongating

the stem of the folded DNA-hairpins. The base structure to which the additions were made was designed to fold into a 9C-hairpin with a melting temperature just above ambient temperatures.

Additionally, by choosing the final base pair in the stem as G-C or T-A, the predicted structure can be altered. For T-A ended hairpins, the lowest free energy configuration does not have the final base pair hybridized. For hairpins with the same sequence otherwise, but G-C as a final base pair, the entire double stranded stem is expected to be closed.

Results

To probe the dependency of the optical properties of the produced emitters on the native secondary structure (the 'stem'), 9C-hairpins were designed with differing lengths of the double stranded part. The stems were chosen to avoid formation of other DNA structures where possible. Additionally, when possible, T-A base pairs were preferred over G-C base pairs because cytosine and guanine bases are known to interact more significantly with silver[4,12]. For the initial comparison, emitters were produced from 9C-hairpins with stems five and twelve base pairs long, representative of a 'short' and 'long' stemmed initial hairpin structure respectively.

Twelve base pairs of double stranded DNA would lead to a melting temperature of the native hairpin structure of 45°C [15], significantly over room temperature. Secondly, because the length of the DNA double helix which stabilizes the hairpin structure can be approximated to be 1 nm per 3 base pairs in length[16], we would expect the it to be around 4nm long. Twelve base pairs would therefore appear to be a reasonable initial representation of a 'long' stem.

Emitters with a five base pair stem were chosen to be the shortest possible representation, because the four base pair equivalents would be expected to no longer have the 9C-hairpin as its lowest energy configuration, having three more likely possible folded DNA structures. Additionally, the melting temperature of these would be expected to be around 17 °C, below ambient temperatures. In comparison, the five base pair native hairpin would be expected to melt around 25 °C, and is most likely to have folded into the hairpin shape before initiating Ag-DNA formation.

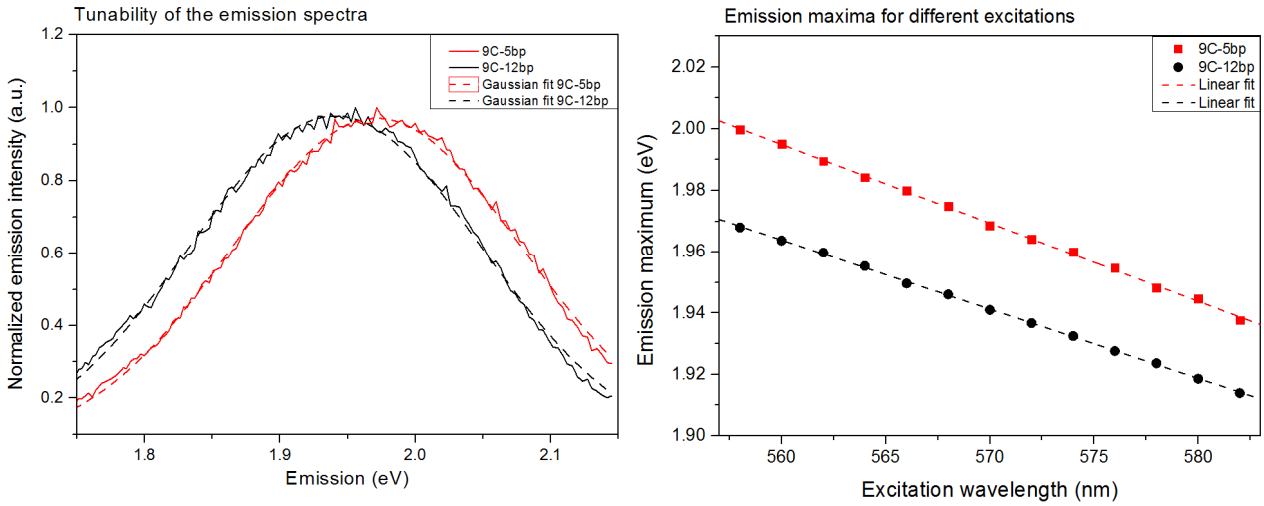

Figure 2: Emission spectra (left), and the position of the emission maximum (right) of Ag-DNAs produced from 9C-hairpins with five ('9C-5bp', red) and twelve ('9C-12bp', black) base pair stems. Measurements were performed on the samples in solution at room temperature, through use of a fluorimeter. The emission spectra result from 570nm excitation. Dashed lines indicate Gaussian fits of the data, yielding peak positions of 629nm (9C-5bp) and 639nm (9C-12bp), or a shift of 30meV.

Emission spectra of the two 9C-variants in solution are shown in Figure 2. Both emitters produce Gaussian spectra of similar widths when excited with 570nm light. However, the emission maximum of the short stemmed example (9C-5bp, red) is significantly blue shifted, by around 10nm.

When the excitation wavelength is varied (Figure 2, right), we observe a significant change in the maxima of the emission spectra. This dependency is present because of substantial inhomogeneity within the emitter distribution, as is also evident from the broadness of the peaks in Figure 1. These types of DNA hairpins are known to stabilize individual Ag-DNAs which are spectrally different. These differences are likely to be the result of different direct environments, or slightly different structural conformations between emitters[9].

We note however, that the dependency on the excitation wavelengths is similar for both the short- and long-stemmed variants discussed, linear fits (Figure 2, right, dashed lines) yielding 2.5 meV/nm and 2.3 meV/nm respectively. In other words, the shift between the emission maxima of the two variants has a low dependency on excitation wavelength. Additionally, the width of the emitter distribution, or the spectral diversity within the emitter ensemble, appears to be similar when a long or short stemmed hairpin is used for Ag-DNA formation.

To explore the full tunable range of the emitters, the length of the stem was varied between five and eighteen base pairs. Apart from the differences arising from the length of the stems, emitters from hairpins ending with a G-C base pair were observed to behave significantly differently to their T-A ended counterparts.

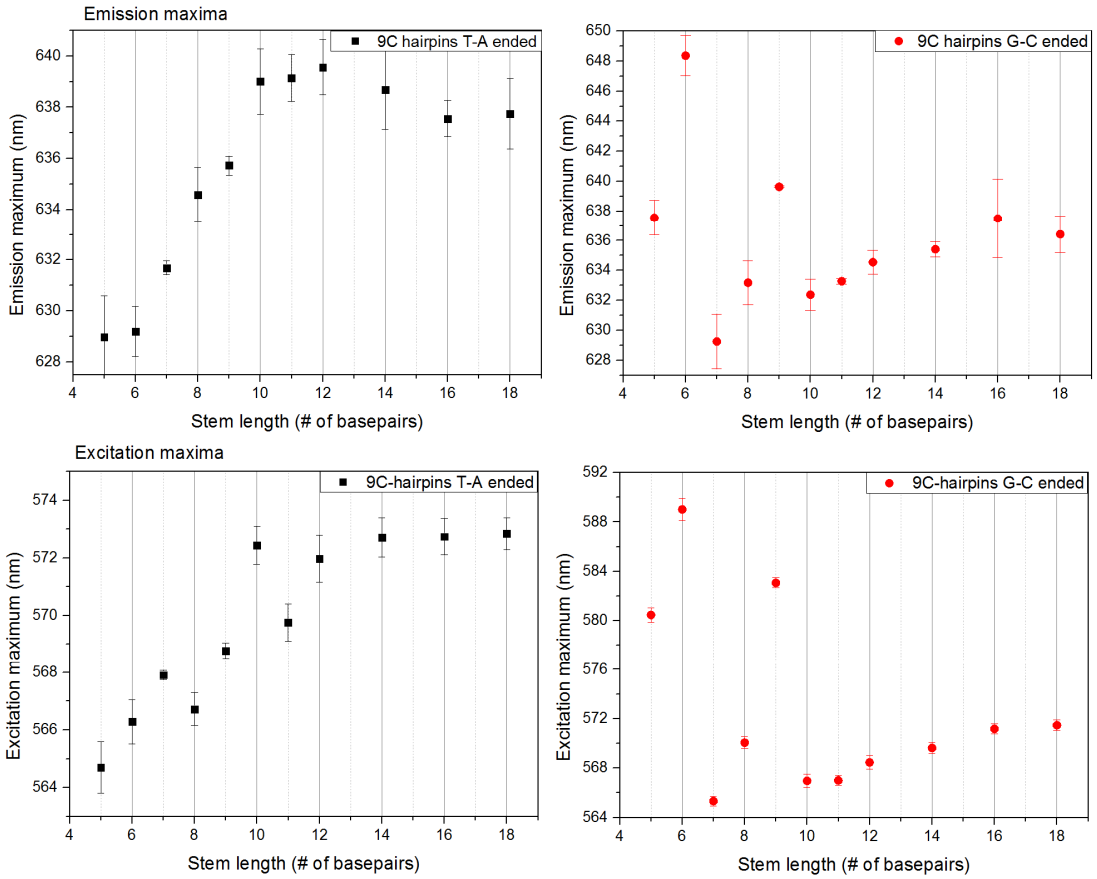

Figure 3: Emission maxima (top) and excitation maxima (bottom) of 9C-hairpin Ag-DNA's with varying stem lengths. Hairpins of which the end, consisting of the 5' and 3' ends of the strand, is a T-A base pair (left, black) are plotted separately from G-C ended counterparts (right, red). The data points are produced through Gaussian fits of spectra taken on emitter ensembles in solution, for 570nm excitation.

Modifying the length of the hairpin stem results in tunable optical properties in the formed emitter distribution, as shown in Figure 3.On the top left graph, we note that hairpins ending in a T-A base pair show a clear trend towards longer wavelengths when the stem is longer. A tunable range for the emission peak between 629nm and 640nm is achieved through lengthening or shortening the stem between five and twelve base pairs.

Hairpins of which the end of the strands is represented by a G-C base pair (top right) were observed to be vastly more irregular for stems shorter than seven base pairs in length. These shorter stems produce several longer wavelength distributions with an emission maximum at wavelengths up to 647nm.

Guanine, and cytosine bases in particular are known to be most involved in interactions with silver[4,12]. If the added G and C bases are allowed to interact with the silver cluster directly, they would have a significant effect on emitter formation. However, the persistence length of double stranded DNA will, depending on conditions, be in the tens of nanometers range[17], much longer than the 2-6nm stems used [16]. The double stranded stem bending far enough to allow the final base pair to interact with the silver cluster can therefore be considered impossible. We may therefore conclude that the double stranded

structure does not maintain its native shape for these short-stemmed hairpins during emitter formation. The final base pair would be much more capable of interacting with the cluster within the 9C-loop directly if the stem is disturbed into a single-stranded state[18].

For G-C ended hairpins with longer stem lengths, ranging between seven and eighteen, a fine-tunable range between 629nm and 636nm is observed, slightly blue shifted relative to their T-A ended equivalents.

Simultaneous changes in excitation behavior

A change in the emission wavelengths can potentially be the result of a change in the resonance of the Ag-DNA complexes as a result of a change in the DNA encapsulation. Alternatively, this shift can be attributed to a change in Stokes shift due to a different number of available vibrational modes when the DNA strand is longer. For the latter, we would expect the excitation path to remain relatively unchanged. To answer this question, we compare the excitation spectra of the 9C variants discussed, as shown in the bottom half of Figure 3.

Comparing the same five and twelve base pair examples used in Figure 2,we note that the shift in the excitation maximum of these two is 28meV, and is comparable to the shift in the emission spectra, 30meV. From the dependency of the excitation maximum on stem length, we note that the behavior is similar to the changes in the emission spectra. This shows that the resonance on which the distribution of the stabilized Ag-DNA complexes is centered can be significantly changed through shortening of the double stranded stem of the DNA hairpins. These changes account for the shift in the emission spectra when the stem is changed, and point towards a more structural change in the conformation of the cluster and/or its DNA ligand.

Because the melting temperatures of the native hairpins are significantly higher than ambient temperatures when the stem is over five base pairs long, we would not expect the addition of a base pair to change the initial DNA structure significantly. We would, however, expect the double helix to be more rigid when it is longer, making it less likely to be disturbed from its initial state during emitter formation. A rigid secondary structure could have a follow-on effect on the dynamics of the 9C-loop as it encapsulates the cluster through limiting its degrees of freedom, leading to a more loosely wrapped silver cluster. When the stem is disturbed, however, a direct effect on the size of the cluster through squeezing, or the proximity of the DNA bases may result in a change in the optical activity of the fluorescent Ag-DNAs.

In other words, the blue shift in shorter stemmed variants may be the result of a more tightly encapsulated silver cluster in the resulting Ag-DNA complex when the native double stranded stem becomes unstable during emitter formation. This is supported by the unpredictable optical properties of the emitters formed out of G-C ended hairpins when the stem is short. If this is the case, adding rigidity to the native secondary structure could lead to emitters with a more well-defined hairpin-like structure, potentially resulting in a less tightly wrapped silver cluster.

If the spectral differences are indeed caused by a tightening of the DNA around the cluster, altering the wrapping of the cluster, even after the emitters have been formed, would be expected to have an effect on its optical properties.

Using temperature to change the DNA-environment

An increase in temperature can be used to change the dynamics of the DNA surrounding the silver cluster, and can give us an insight into effects on the optical properties of the emitters by the state of the DNA encapsulation. By heating up the DNA hairpins, we would expect the structure directly around the cluster to become more dynamic, and the cluster to become more loosely wrapped. One would expect any effects of the direct DNA environment on the clusters in shorter stemmed hairpins to be mitigated at higher temperatures as a result.

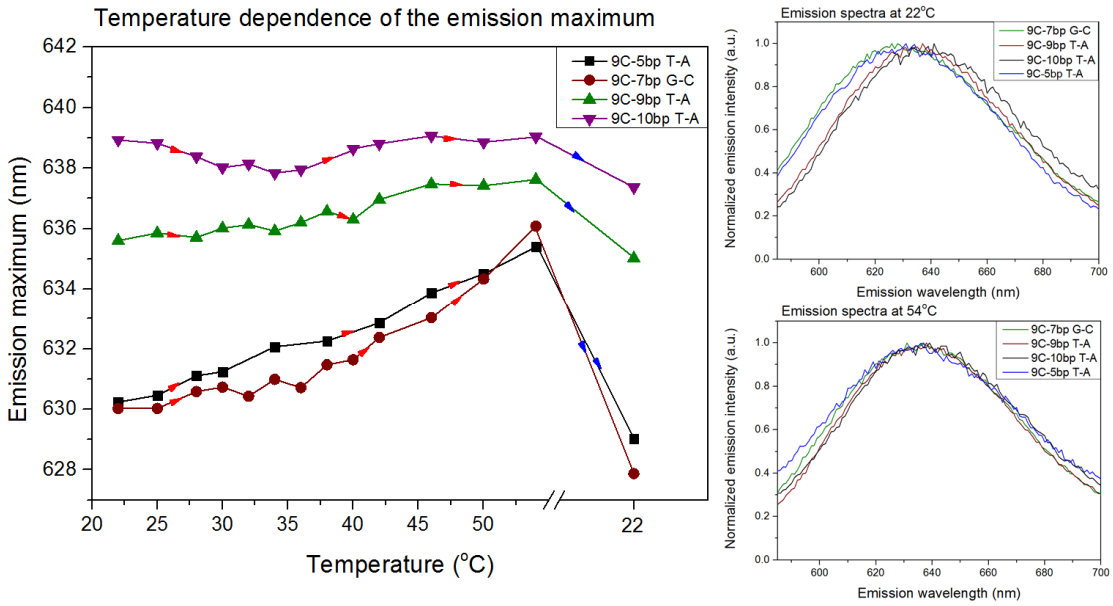

Figure 4: Progression of the position of the emission maxima during a temperature increase. '9C-5bp T-A' (black), '9C-7bp T-A' (brown), '9C-9bp G-C'(green) and 9C-10bp T-A (purple) emitters were used, with room temperature emission maxima of 630nm, 630nm, 636nm and 639nm respectively. The data points are the result of Gaussian fits on emission spectra taken in solution. Red arrows indicate heating of the sample solution, blue arrows indicate the sample cooling back down to ambient temperatures. The two graphs on the right show the convergence of the emission spectra of the emitters at high temperatures (bottom) relative to room temperature measurements (top).

The emission peak of the emitter distribution changes significantly when the temperature of the solution is changed, as shown in Figure 4. We observe that the emission maximum of the longest wavelength emitters, '9C-10bp T-A', remains relatively unchanged. The initially slightly blue shifted '9C-9bp T-A' emitter red shifts towards the emission maximum of the longer stemmed variant. Emitter distributions with a larger inherent blue shift, '9C-7bp G-C' and '9C-5bp T-A', show a more significant change in emission spectrum when the temperature is increased. At 54 °C, the three variants have converged to be within a 4nm spectral range, as shown in the emission spectra in Figure 4.

The spectrum representing '9C-5bp T-A', the emitter with the shortest stem, seems somewhat broadened at higher temperatures. This effect is likely to be caused by larger instabilities as a result of the melting of the Ag-DNA complex, which this emitter should be more sensitive to, because of its short DNA strand.

The samples spectrally revert to close to their initial state after cooling back down to ambient temperatures. Additionally, the emission from the samples used never dipped below 50% when heated to 54 °C, as measured by the area of Gaussian fits to the emission spectra. This can be considered surprising, due to the relatively low expected melting temperatures of the native hairpins, especially for the '9C-5bp T-A' case (25 °C[15]). It would appear that Watson-Crick base pairing in the stem is not the only contribution to the thermal stability of the resulting emitter structure. The addition of silver, and subsequent silver cluster formation, seem to lead to final configurations with a higher melting temperature. Silver has been known to mediate non Watson-Crick base pairing[19],with formation of C-Ag^{+}-C bonds in particular. The presence of silver ions and the wrapping of the DNA loop around the silver cluster are therefore likely to be large contributions to the rigidity of the structure.

Additionally, because shorter-stemmed variants typically yield emitter distributions centered on a shorter wavelength (Figure 3), a red-shift in the emitters at higher temperatures is unlikely to be caused by the breaking of individual base pairs shortening the stem. We would therefore expect the temperature dependency to be dominated by the silver-mediated structure in particular, and be representative of the effect of the DNA environment of the silver cluster on the optical properties of the emitters.

A change in the direct cluster environment is therefore a likely explanation for the differing optical properties of the emitter variants. If the blue-shift in the shorter-stemmed cases is indeed caused by a tightening of the DNA around the silver cluster, we expect the emitters' activity to converge towards longer wavelengths at higher temperatures, as seems to be the cage.

Optimizing Ag-DNA formation

DNA strands of the same length and sequence are known to stabilize multiple sizes and shapes of silver cluster, and even multiple species of fluorescent Ag-DNA [12,13]. Specifically, the 9C-hairpins under discussion allow formation of two dominant fluorescent species in the red and green parts of the spectrum, as is evident from Figure 1. Additionally, as has been mentioned (Figure 2), the emitter distributions are relatively broad. The broadness of the distribution can be considered undesirable for the use of these emitters as fluorescent labels, on a few- or single fluorophore level in particular, because the exact optical properties of individual emitters become impossible to accurately predict[9].

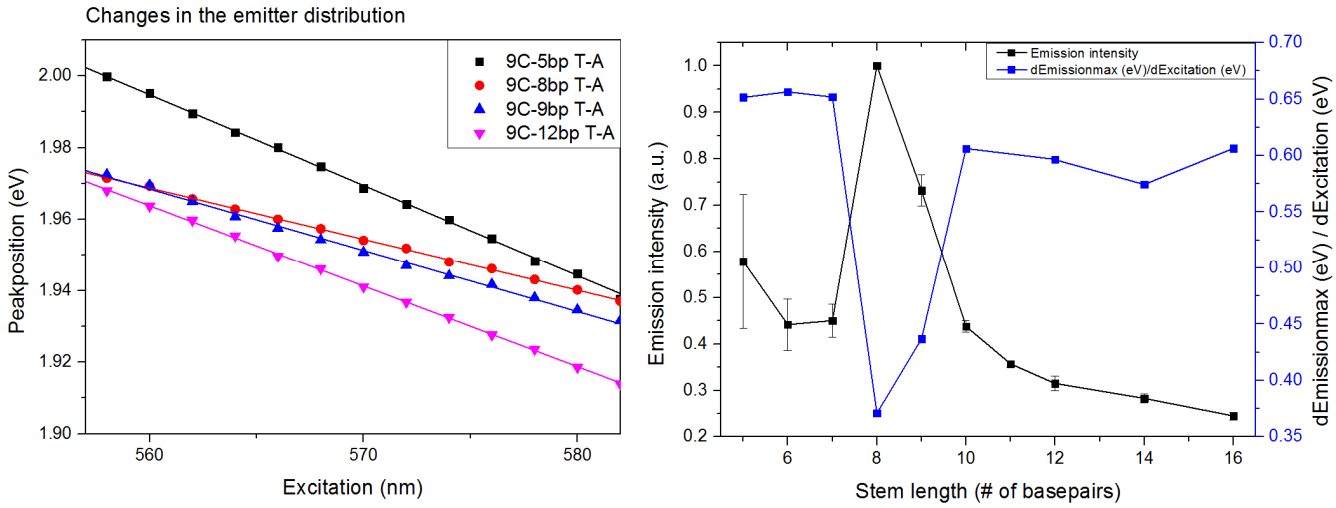

Figure 5: Emission maxima of 9C-hairpin Ag-DNAs with varying stems, as a function of excitation wavelength (left). The blue data points on the right constitute the slope of linear fits to the excitation dependency of the emission maximum. Also included is the emission intensity, as represented by the area of Gaussian fits to emission spectra (right, black).

The variability in the emitter distribution is shown in Figure 5. Again, the variation in the emission maximum for different excitations is a measure of the heterogeneity of the emitter distribution. The results show a decreased dependency on the excitation wavelength for eight and nine base paired 9C-hairpins. Additionally, the emission intensity (right, black) is significantly larger around these stem lengths. We would therefore expect the eight or nine base pair hairpins to represent the most suitable initial environment for stabilization of these red fluorescent Ag-DNAs, yielding the most bright and spectrally pure emitter ensemble.

Conclusion

To summarize, fluorescent Ag-DNAs have been produced from 9C-hairpins with double stranded 'stems' of varying length and sequence. The optical properties of the emitters that form can be changed controllably using this method. A simultaneous change in both the emission and excitation maxima of the distribution shows that the fluorescent emitters have a similar Stokes shift, but become centered on a different resonance.

The addition of a G-C base pair to a short stem leads to a large change in the emitter distribution, leading us to conclude that the stem in short-stemmed emitters is likely to be disturbed during cluster formation. We therefore propose attributing the spectral differences to more tightly or loosely wrapped DNA environment around the cluster in its final configuration. Convergence of the optical properties of the emitter distributions at higher temperatures, when the cluster is forcibly more loosely wrapped, supports this explanation.

Finally, the base pair-by-base pair method of tuning the emitter structure has been used to optimize the effectiveness of production of these red fluorescent emitters. Use of the proposed eight base pair stem leads to an increase in yield by a factor of 2-3 compared to the other studied variants, and a halving of the spectral width of the distribution.

Chapter 2 - Fluorescence quenching through energy transfer to DNA-stabilized few-atom silver clusters

Nano Surface Energy Transfer (NSET) from fluorescent dyes to metal particles represents a useful tool as a nanometer scale ruler, with greater spectral flexibility, and a greater operating range than typically used FRET-pairs. Additionally, the emergence of DNA as a widely used scaffolding tool has led

to greatly increased accuracy of placement, opening up the single nanometer resolution for design and experimentation. Because DNA can also be used as a ligand to stabilize metal nanoclusters, creating signaling and distance measuring tools based on fluorescence quenching through NSET becomes an attractive possibility. We now report on the fluorescence quenching of commercial dyes throughout the visible range through synthesis of DNA-stabilized few-atom silver clusters (Ag-DNA). A fluorescent dye is positioned on the end of a DNA strand, after which a quenching efficiency of up to 85% is achieved by silver cluster synthesis, with very large chemical yields. We utilize these constructs to observe a particularly strong dependency on the size of the metal particle in this range.

Introduction

When analyzing small structures, especially inside living biological systems, distances rapidly surpass the limits of typically available forms of microscopy. For moving objects in particular, the ability to discern features on a scale of individual nanometers is generally impossible. As such, deriving distances from indirect techniques such as optical interactions, EPR or NMR, is an often used and expanding field of research. These techniques are often limited by an inability to introduce and maintain modifications such as spin labels to complicated biological systems in an in vivo environment.

Therefore, the chemical stability and small size of fluorescent labels make interactions between these a commonly used technique for measuring proximity. For example, Förster Resonance Energy Transfer (FRET)[20] is a typically used phenomenon in these experiments, allowing the detection of the proximity of two objects within 5-7 nanometers through an on/off fluorescence signal.

To combine the ability to measure finer distance variations on the order of nanometers with the stability of fluorescent labels used in FRET, Nano Surface Energy Transfer (NSET) from a fluorescent dye to a metal surface is a potentially valuable tool[21–25]. In this process, the energy from an excited dipole, such as a fluorescent dye, can be transferred to dipoles on the metal surface represented by free conduction band electrons in the metal. Utilizing this effect, the proximity of a fluorescent dye to a metal surface can potentially be determined on a scale of individual nanometers, through the measurement of quenching of the fluorescence. The large quenching efficiency, the well-defined distance dependency of $1/r^{4,}$ and typical working distance of 10-15 nm makes it particularly applicable to biology such as in protein-interactions or the activity of nucleic acids[21,26,27].

The difficulty in NSET experiments in the past has arisen from the challenges involved in incorporating metal surfaces in experimental systems, due to the typically large size of metal nanoparticles, as compared to fluorescent dyes. However, in recent years, DNA has become a valuable tool in positioning objects on a nanometer scale, opening up the potential to study the NSET process through double stranded DNA spacers[28]. Additionally using single stranded DNA (ssDNA) as a ligand, DNA-encapsulated few atom silver clusters (Ag-DNA)[29] can be easily and reliably produced, positioned[30], and used in various environments, including in living biological systems[31]. Ag-DNA are typically produced by introduction of free silver ions to a solution of ssDNA templates, followed by chemical reduction to create few-atom silver clusters containing uncharged atoms, surrounded by silver ions bound strongly to the DNA bases. The resulting silver clusters are typically 5-20 atoms in size[10,11,14], whereby the size and shape strongly depend on the stabilizing ssDNA stand[4,13,32], and can be distinctly rod-shaped[11]. It has

been shown that after synthesis, the produced silver clusters can be easily attached to other objects using DNA hybridization[33] Alternatively, by incorporating ssDNA templates into a structure, the silver clusters can directly be synthesized onto larger structures[30]

This allows for the creation and positioning of metal surfaces potentially exhibiting NSET with particle sizes of one nanometer or less. Additionally, the DNA used as a ligand can easily be modified and bound to other objects[30,33], opening up a multi-functional tool for the measurement of distances, in particular in living or otherwise moving systems. Additionally, the inherently strong fluorescence of the Ag-DNA themselves means these structures represent dual-color assemblies, further expanding their potential range of use.

One aspect of the NSET interaction that has often been hard to quantify in theoretical work, but more recently has attracted interest experimentally[21,23] is a potential dependency on particle size. Due to the large amount of screening of the dye's dipole potential at the metal surface, it would not be surprising for the interaction to be significantly weaker for particles only a few atoms in size. Due to the difficulty in producing and positioning such small clusters, it has been difficult to see these effects historically, but the unique properties of Ag-DNA will open up investigations such as these more easily.

Materials and Methods

DNA strands were purchased from Integrated DNA Technologies with standard desalting, and used without further purification. Strands were prepared and mixed in 20 mM NH4OAc, and silver cluster synthesis was performed through addition of AgNO3 (99.9999%, Sigma Aldrich) in a 12.5:1 AgNO3:DNA ratio unless stated otherwise. Afterwards, reduction was performed with NaBH4 (99%, Sigma Aldrich) in a 6.25:1 NaBH4:DNA ratio, after a 30 min incubation. Samples were allowed to stabilize their fluorescence for 2 hours after reduction. Bulk fluorescence measurements were then performed by collecting emission spectra on a Cary Eclipse fluorimeter (Varian). Lifetime measurements were carried out in a custom-built confocal microscopy setup, utilizing a 639 nm pulsed laser at a 20 MHz repetition rate. Imaging and measurement were performed using a 100X oil immersion objective, NA 1.4 (Zeiss). The pinhole size was 75 µm. The data was captured using a photon-counting PC-board (TimeHarp 200, PicoQuant), and analysis was performed using SymPhoTime software (PicoQuant).

Results

To show that NSET activity can be observed for silver particles only 10-20 atoms in size, we have produced hybrids of a fluorescent dye and silver clusters on individual ssDNA templates. The used DNA strand (19b) has been utilized to stabilize fluorescent silver clusters of around 10 atoms in size[10], and is likely to produce a range of silver products of various shapes and sizes. Although the exact DNA conformation as it stabilizes the silver cluster is unknown, the limited total length of the 19-base DNA strand (13 nm[18]) allows us to position the fluorescent dye within NSET range by simply having it be bound to the DNA template prior to synthesizing the cluster.

To exhibit the availability of the technique for dyes with resonances throughout large parts of the visible range, and to avoid a dependency on dyes with a specific chemical structure, various commercial dyes are used with excitation maxima ranging from 521nm (TET) to 650nm (Cy5).

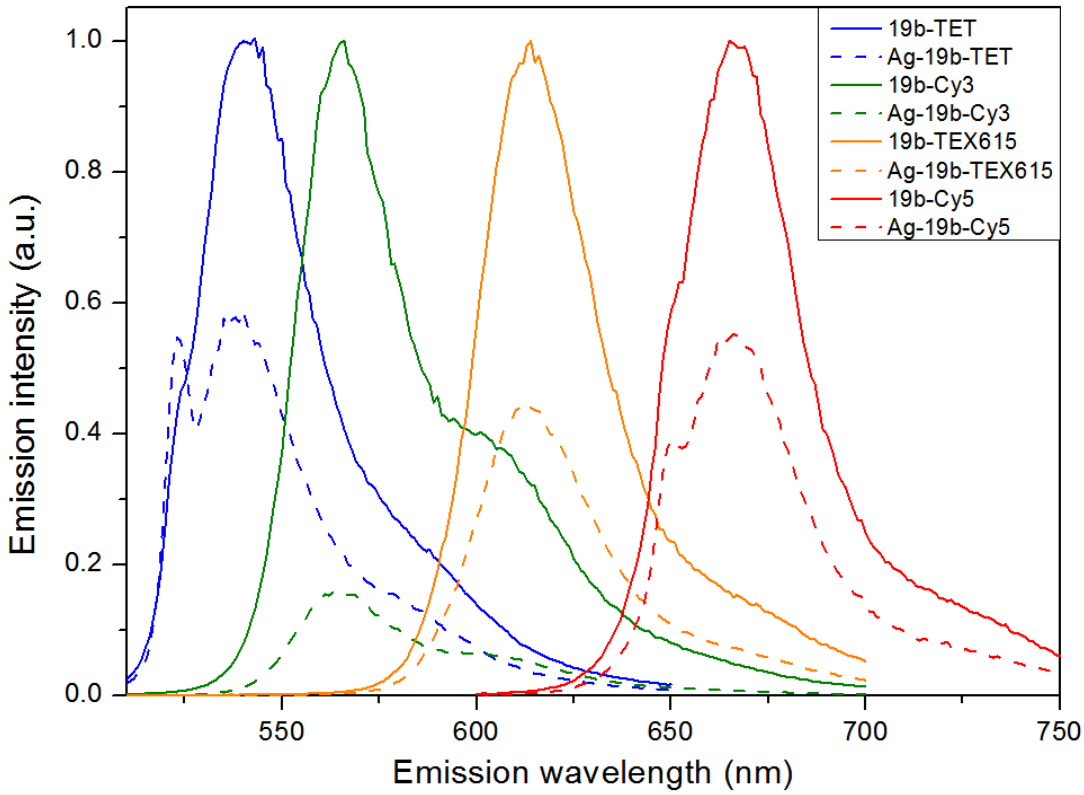

Figure 1 Fluorescence emission spectrum from TET (blue), Cy3 (green), TEX615 (orange) and Cy5 (red) attached to the 19b ssDNA strand. Dashed lines represent the same dyes after performing synthesis of few-atom silver cluster on the attached strand. Excitations were at the respective maximal excitation wavelengths of the respective dyes. The data is normalized with respect to any small changes in absorption measures separately.

Figure 1 shows the change in emission intensity of the fluorescent dyes upon silver cluster synthesis. Simultaneously, relatively minor (<13%) changes in absorption were observed, likely due to the different chemical environment or conformational changes induced by silver cluster synthesis. The data in Figure 1 has been normalized with respect to any measured changes in absorption, meaning the results represent changes in the average quantum yield. The resulting drops in yield range between 42% (TET) and 85% (Cy3). All dyes used in our experiments exhibited significant quenching when the silver cluster has formed. The large difference in intensity observed can easily be detected in typical fluorescence measurement devices, and opens up the possibility to see the changes in emission in fluorescence microscopy.

In our results, it is noteworthy that the quenching efficiency is significantly larger for the Cy3 dye. It is expected that the NSET interaction can increase significantly due to a metal particle's plasmonic

resonance. Therefore it is likely that the energy transfer from Cy3 is so strong because it overlaps with the resonance observed on the fluorescent clusters stabilized on these strands[10].

For determining quenching efficiencies, bulk measurements of fluorescence and absorption as shown in Figure 1 are typically inaccurate due to changes in the chemical environment. Additionally, bulk measurements measure the entire dye distribution, and do not distinguish between the various products of silver cluster synthesis, including any strands that failed to stabilize a silver cluster.

Fluorescence lifetime measurements are a more sensitive method of measuring changes in quantum yield, allowing for accurate single molecule measurements of the quenching efficiency. To facilitate this, we immobilize the ssDNA-mounted dyes in PVA to excite individual molecules, and determine the change in fluorescence lifetime upon silver cluster synthesis.

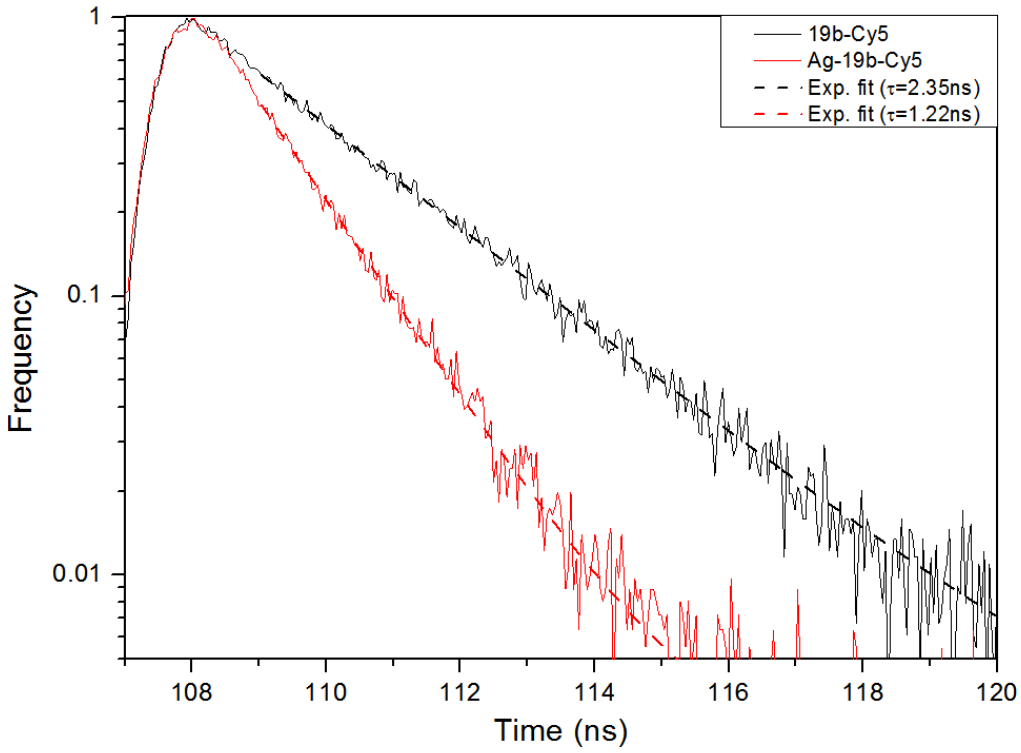

Figure 2: Fluorescence lifetime measurements on a single Cy5-dye attached to the 19b ssDNA strand (black), and after synthesis of a few-atom silver cluster (red). Samples were immobilized in PVA to be able to excite individual dye molecules. The dashed curve represents exponential decay fits to the data to determine the fluorescence lifetime.

A typical change in fluorescence lifetime of a Cy5-dye on the ssDNA template upon silver cluster synthesis is shown in Figure 2. To ensure that the measurements represent individual dye molecules, intensity time traces are taken simultaneously to ensure one-step photobleaching.

To determine the quenching efficiency, we define the quantum yield (Q) from the rates of excited state decay (k) and radiative decay (k_r):

$$Q = \frac{k_r}{k}$$

and defining the quenching efficiency as the relative change in quantum yield:

$$\eta_q = \frac{Q'}{Q} = \frac{k}{k'} = \frac{\tau'}{\tau}$$

With τ', τ the measured quenched or unquenched fluorescence lifetimes, as determined by exponential fits. In this approximation, we assume that the change in emission is due to the opening up of additional non-radiative decay paths only, meaning the radiative decay rate is unchanged. The resulting quenching efficiency of the dye-silver cluster pair shown in Figure 2 is 48%.

The fluorescence lifetime quantifies any radiative and non-radiative decay paths available, making it particularly sensitive to the dye's local environment. Therefore, the measurement is repeated for 200 individual molecules, leading to fluorescence lifetime distributions shown in Figure 3.

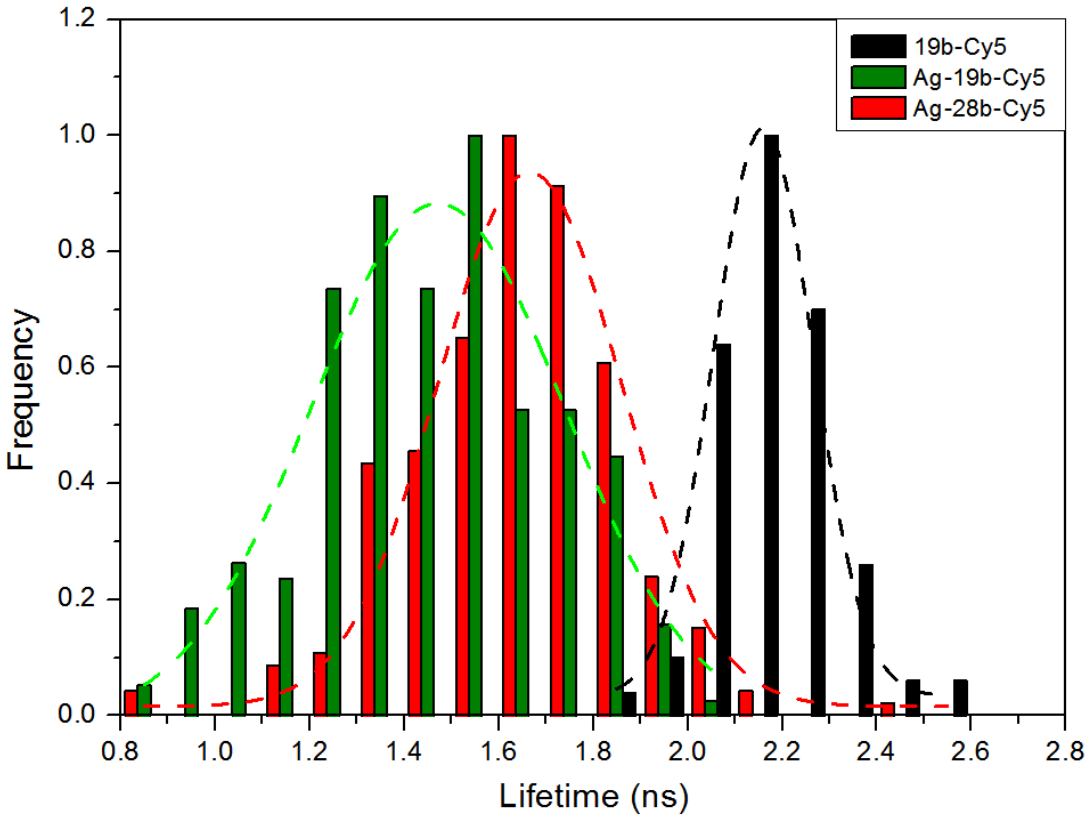

Figure 3: Distributions of measured fluorescence lifetimes from Cy5 dyes attached to the 19b ssDNA strand immobilized in PVA (black), and after synthesis of a few atom silver cluster (green). The same experiment was performed while using a different ssDNA host to stabilize the cluster, 28b (red). Centers of the distributions are determined through Gaussian fits (dashed lines) as 2.24ns (19b-Cy5), 1.42ns (Ag-19b-Cy5), and 1.66ns (Ag-28b-Cy5).

Notably, nearly all quenched Cy5-dyes (Figure 3, green) exhibit fluorescence lifetimes outside of the usual range of lifetimes shown by the unquenched dyes (Figure 3, black), indicating a large chemical yield of silver cluster synthesis. For comparison, a longer DNA strand, Ag-28b[11], is included in the experiment (Figure 3, red) to exclude any effects specific to the 19b strand, and vary the position of the dye with respect to the formed silver cluster.

For the Ag-19b-Cy5 pairs, we observe an average quenched fluorescence lifetime of 1.42ns, as compared to 2.24ns for the DNA-bound dyes used in the control, for an average quenching efficiency of 37%. Measuring the quenching efficiency through bulk fluorescence produced a similar number (41%), allowing us to attribute the change in emission almost entirely to the quenching interaction. This is further evident from the lack of detected fluorescent lifetimes corresponding to the control after cluster synthesis.

When utilizing a larger DNA strand, Ag-28b, to stabilize the silver cluster, we observe the same quenching interaction, with an average fluorescence lifetime of 1.66ns. This corresponds to an average quenching efficiency of 26%, significantly lower than the equivalent for Ag-19b, and again comparable to the total reduction in fluorescence as measured in bulk (31%).

This difference in quenching efficiencies between Ag-19b and Ag-28b is likely due to the length of the DNA strand, 19 bases vs. 28 bases, or 13 nm vs. 19 nm, causing the dye to be positioned further away from the cluster on Ag-28b.

Another effect that is visible in Figure 3 is the broadening of the distribution of fluorescence lifetimes due to the quenching. This implies that the strength of the quenching interaction varies significantly between the individual pairs of dyes and silver clusters.

One potential factor to the NSET interaction that can explain this, and that we can explore using our few-atom clusters, is the dependency on the size of the metal particle. Given the screening of the dipole potential in the metal surface limiting the overlap with the electronic wave functions, it is not unlikely that for particles this small in size the strength of the quenching is size-limited. To examine this, we increased the size of our particles by increasing the number of silver ions per DNA strand from 12.5 to 22.5.

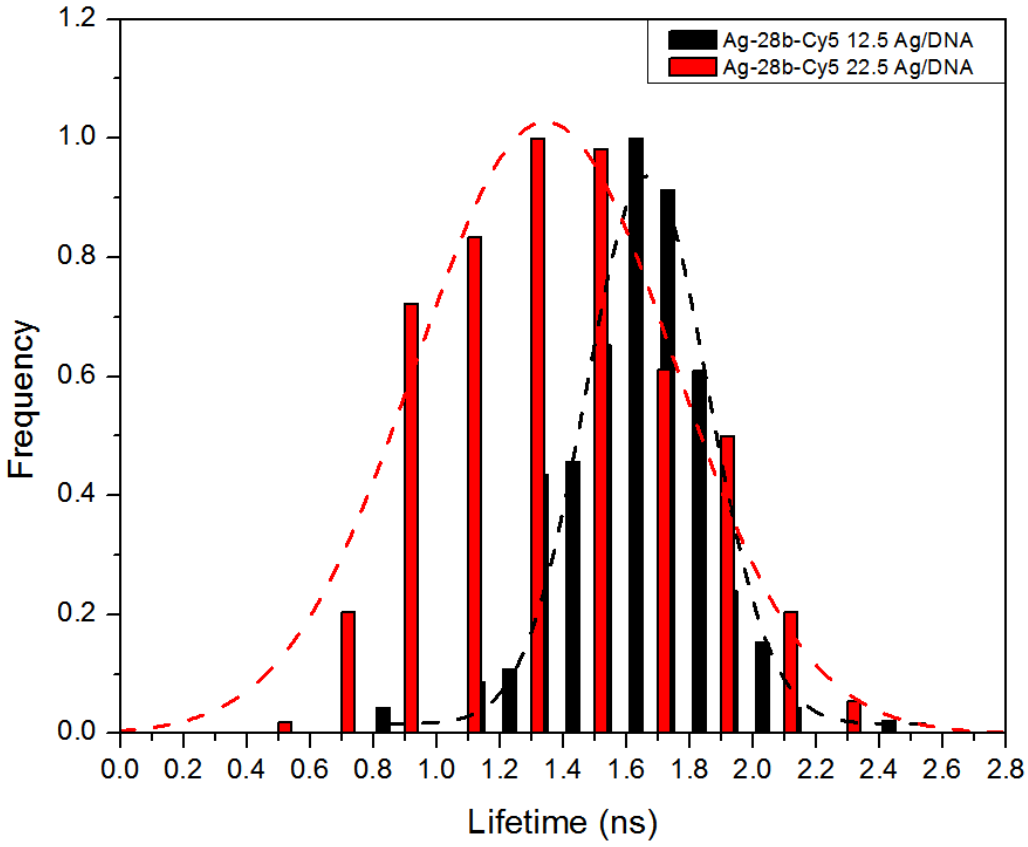

Figure 4: Distributions of measured fluorescence lifetimes from Cy5 dyes attached to the 28b ssDNA strand immobilized in PVA after synthesis of a few-atom silver cluster, at Ag/DNA ratios of 12.5 (black) and 22.5 (red). Dashed lines represent Gaussian fits to the data, yielding centers of 1.67 ns (12.5 Ag/DNA) and 1.34ns (22.5 Ag/DNA), and widths of 0.44 ns and 0.98 ns respectively.

In Figure 4, we compare the distribution of fluorescence lifetimes of Cy5 dyes in the proximity of silver clusters stabilized by the 28b sequence. The center of the fluorescence is shifted from 1.67 ns to 1.34 ns when the silver content is increased, and the FWHM of the distribution increases dramatically from 0.44 ns to 0.98 ns. The average quenching efficiency therefore increases from 26% to 40%.

Discussion

In our experiments we show fluorescence quenching of various dyes throughout the visible range, through synthesis of few-atom silver clusters on an attached strand of ssDNA. In bulk measurements (Figure 1), we note that the decreased fluorescence is significant for all dyes used, and relatively small changes in absorption show that the change corresponds to a quenching of the fluorescence emission. The smallest amount of quenching was observed when using the TET dye (41%), and the effect is strongest for Cy3 (85%). From the established theory, we expect that the strength of the quenching increases linearly with the frequency of the resonance, but stops being effective for large frequencies. This is due to the velocity of the oscillation of image dipoles being limited in the metal. It is true that our shortest wavelength dye (TET) exhibits the least amount of quenching, but we do not believe this an

accurate representation of the frequency dependency because of the large differences in the chemical structures of the dyes.

Because of this, it is difficult to determine the significance of the strong quenching of the Cy3 dye, but it must be noted that its emission overlaps with the emission spectrum of the fluorescent Ag-DNA structures stabilized by this strand[10]. It is therefore expected that the increased absorption cross section near the plasmonic resonance significantly increases the clusters' efficiency as acceptors. Notably, because ssDNA strands have been shown to produce a wide range of different clusters with various resonances, this suggests that it can be possible to tune the silver cluster's resonance to match the dye to enhance the quenching efficiency.

In single-molecule fluorescence lifetime measurements on Cy5 dyes close to the metal surfaces, we confirm the fluorescence quenching behavior through the decreased fluorescence lifetime. We further note that the distributions of dyes appears entirely quenched (Figure 3) after the synthesis of two types of silver clusters, with no significant presence of unquenched dyes. The strength of the quenching as determined through the change in fluorescence lifetime (37% for Ag-28b and 26% for Ag-19b) is close to the total observed change of fluorescence in bulk (41% for Ag-28b and 31% for Ag-19b). From this we conclude that close to the entire distribution of DNA strands has stabilized a silver cluster capable of quenching the fluorescence from the dye.

The width of the distribution of lifetimes is significantly larger after the clusters have been synthesized as well. This implies that the strength of the quenching interaction is not a constant throughout the distribution.

When the silver content is increased to stabilize larger silver clusters (Figure 4), we observe a significant increase in the quenching efficiency and width of the distribution of lifetimes. This behavior is consistent with the expected broader distribution of on average larger particles, if the quenching depends directly on the size of the particle. Therefore, we suggest that the strength of the NSET interaction is likely to have a particularly strong dependency on particle size for few-atom clusters such as these.

Conclusion

In this work, we exhibit the quenching of fluorescent dyes throughout the visible range, through synthesis of a few-atom silver cluster in close proximity on an attached ssDNA strand. In doing so, we achieve easily detected quenching with efficiencies up to 85%, whereby the chemical yield of cluster synthesis appears to be close to 100%.

The results show the ease at which energy transfer mechanisms to these small metal surfaces can be studied using DNA-stabilized few atom clusters, and open up further experimentation to study both the NSET process and its applications. By increasing the size of our clusters through the silver content, we observe a significant increase in quenching efficiency, suggesting that energy transfer has a strong dependency on the size of the metal cluster in this range.

Through our experiments, we find that the few-atom clusters in Ag-DNA, which can be easily positioned through the connected DNA strand, and are small enough to incorporate into complex systems, can

potentially perform a useful role as nanoscale rulers. Additionally, the known tunability of the particle size and plasmonic resonance can allow for the NSET interaction to be optimized for specific applications.

Appendix A - Observations on Ag-DNA synthesis/quenching dynamics

From the measurements on the fluorescence lifetimes we note that the average quenching efficiency per dye (Figure 3) is similar to the total quenching observed in bulk solution. We also observe a lack of unquenched dyes in the measured distribution. From this, we can deduce that the chemical yield of silver cluster synthesis seems to be very large, and coverage of the strands with silver appears close to complete.

This is noteworthy due to previous experience with the fluorescent distributions of Ag-DNA[29], predicting that the number of fluorescent emitters that form from the DNA strands is quite low, typically below 5%. Our results suggest that this is a small subset of the silver clusters stabilized by strands, and that in reality almost all the strands have stabilized clusters.

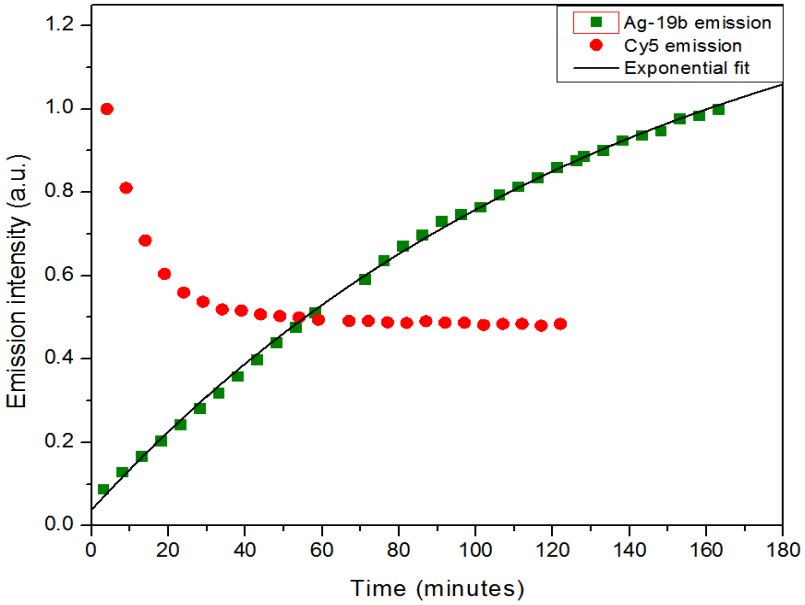

Figure A1: Progression of the fluorescence from a Cy5 dye (red dots) and the fluorescent Ag-DNA 'Ag-19b' over time after beginning silver reduction to form the clusters. The increased fluorescence over time fits a first order chemical reaction as shown by the single exponential fit (black line). The quenching of the dye does not follow the same behavior.

We can observe the difference between the formation of the clusters and of the fluorescent Ag-DNA constructs by looking at the dynamics of fluorescence of a quenched dye and that of the Ag-DNA over time (Figure A1). We note that the quenching rate, or the rate of formation of the clusters, is significantly faster than the rate at which the fluorescent emitters form. The slower formation of fluorescent emitters also follows a first order reaction over the longer timescale.

This behavior, combined with our other results, exhibit the two stages of the formation of fluorescent Ag-DNA: First, the silver clusters stabilize quickly, consistent with our use of a fast reductant in $NaBH_4$. The formation of the fluorescent emitters is a slow process that follows this after the silver clusters have

already formed. It is likely that this process involved the specific positioning of the DNA bases around the silver cluster, in such a way to produce a fluorescent emitter that can be excited.

Appendix B - Increasing silver content to increase particle size

In this work, we suggest that we observe a strong dependence on particle size for the fluorescence quenching of a dye near the metal surface. To study this more closely, the silver content was changed during silver cluster synthesis to change the particle size.

Of course, a direct increase in particle size from the presence of more silver will not always be the case. In particular, when the silver content becomes too high, the expectation is that competition from the formation of other silver products in the solution, away from the DNA, will become more dominant. Additionally, there is only so much silver that the DNA strands can hold based on their limited length. However, we do expect to find a range within which we can change the size of the cluster through modifying the silver content.

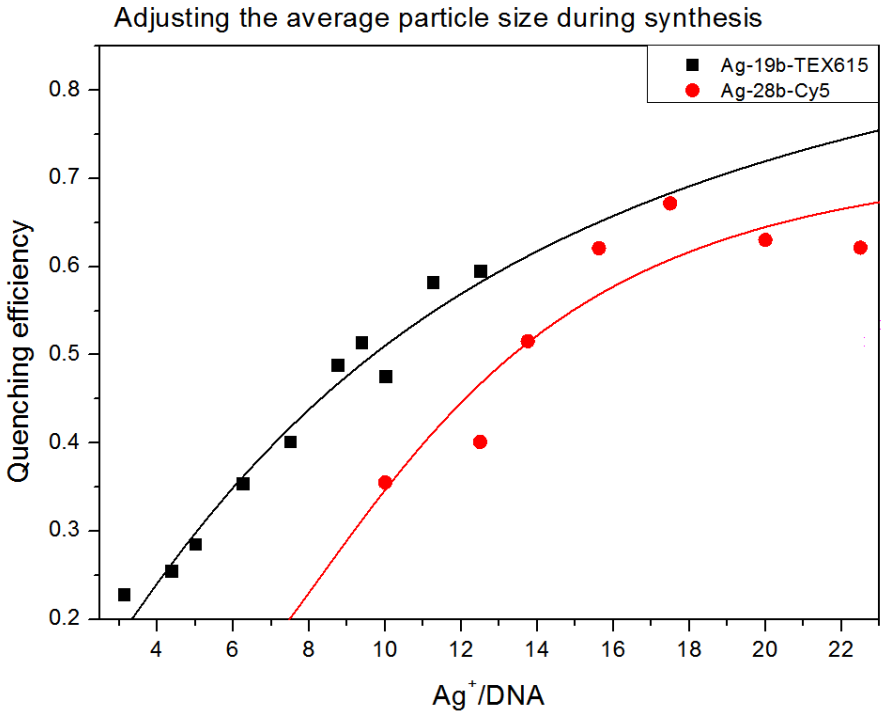

Figure B1: Measured quenching efficiencies in bulk fluorescence measurements, as a function of the silver ion/DNA ratio during silver cluster synthesis. The quenching efficiency is determined by comparing the measured fluorescence intensity to the intensity from the fluorescent dyes without silver present. The dyes used are TEX615 on the 19b strand, and Cy5 on the 28b strand. The black and red lines are Hill equation fits to the data.

When increasing the silver content (Figure B1), we observe a strong increase in the quenching efficiency of dyes attached to the DNA strand. While the Ag-28b construct typically yields less quenching, likely due to the longer strand increasing the distance between the dye and cluster, we note that the

quenching increases particularly strongly with silver concentration. Generally, it can be expected that the longer 28b strand can hold more silver, leading to a larger range of possible cluster sizes.

We use the Hill equation to fit to the data, approximating the system as a fixed number of binding sites on the DNA strand to which the Ag^+ ions can bind. The degree of cooperativity is greater than 1 (1.78 for 19b-TEX615, 2.1 for 28b-Cy5), which implies a degree of cooperative binding in this approximation. We suggest that this is due to the probability of silver clustering in the solution outside of the DNA encapsulation decreasing as the silver in the solution depletes when it occupies the DNA.

Appendix C - Ag-DNA Synthesis procedures and sequences

These are standard synthesis conditions with the aim of maximizing Ag-DNA fluorescence.

For hairpin structures:
20 mM NH_4OAc
50 µM DNA
350 µM $AgNO_3$
100 µM $NaBH_4$

For Ag28b/Ag19b:
20 mM NH_4OAc
50 µM DNA
480 µM $AgNO_3$
240 µM $NaBH_4$

Procedure:
1) Mix the DNA with the silver nitrate
2) Store at 4 degrees for 30 minutes
3) Add freshly prepared NaBH 4 to reduce
4) Store at 4 degrees for at least 8 hours to maximize the fluorescence

Name	Sequence
9C-18b	TAATATAGATACTTACCT CCCCCCCCC AGGTAAGTATCTATATTA
19b	TGC CTT TTG GGG ACG GAT A
28b	CAC CGC TTT TGC CTT TTG GGG ACG GAT A

All 9C-hairpin variants used in this work are the result of shortening 9C-18b and/or replacing the final base pair with a G-C as required.

Bibliography

1. Harbich, W. *et al.* Deposition of mass selected silver clusters in rare gas matrices. *J. Chem. Phys.* **93,** 8535–8543 (1990).

2. Wu, Z. & Jin, R. On the ligand's role in the fluorescence of gold nanoclusters. *Nano Lett.* **10,** 2568–2573 (2010).

3. Devadas, M. S. *et al.* Temperature-Dependent Optical Absorption Properties of Monolayer-Protected Au 25 and Au 38 Clusters. *J. Phys. Chem. Lett.* **2,** 2752–2758 (2011).

4. Petty, J. T., Zheng, J., Hud, N. V & Dickson, R. M. DNA-templated Ag nanocluster formation. *J. Am. Chem. Soc.* **126,** 5207–5212 (2004).

5. Ma, K. *et al.* Base-Stacking-Determined Fluorescence Emission of DNA Abasic. (2012).

6. Richards, C. I. *et al.* Oligonucleotide-stabilized Ag nanocluster fluorophores. *J. Am. Chem. Soc.* **130,** 5038–9 (2008).

7. Sharma, J., Yeh, H.-C., Yoo, H., Werner, J. H. & Martinez, J. S. A complementary palette of fluorescent silver nanoclusters. *Chem. Commun. (Camb).* **46,** 3280–3282 (2010).

8. Vosch, T. *et al.* Strongly emissive individual DNA-encapsulated Ag nanoclusters as single-molecule fluorophores. *Proc. Natl. Acad. Sci. U. S. A.* **104,** 12616–21 (2007).

9. Oemrawsingh, S. S. R., Markešević, N., Gwinn, E. G., Eliel, E. R. & Bouwmeester, D. Spectral Properties of Individual DNA-Hosted Silver Nanoclusters at Low Temperatures. *J. Phys. Chem. C* **116,** 25568–25575 (2012).

10. Schultz, D. & Gwinn, E. G. Silver atom and strand numbers in fluorescent and dark Ag:DNAs. *Chem. Commun.* **48,** 5748 (2012).

11. Schultz, D. *et al.* Evidence for Rod-Shaped DNA-Stabilized Silver Nanocluster Emitters. *Adv. Mater.* **25,** 2797–2803 (2013).

12. Gwinn, E. G., O'Neill, P., Guerrero, A. J., Bouwmeester, D. & Fygenson, D. K. Sequence-dependent fluorescence of DNA-hosted silver nanoclusters. *Adv. Mater.* **20,** 279–283 (2008).

13. O'Neill, P., Velazquez, L., Dunn, D., Gwinn, E. & Fygenson, D. K. Hairpins with Poly-C Loops Stabilize Four Types of Fluorescent Agn:DNA. *J. Phys. Chem. C* **113,** 4229–4233 (2009).

14. Driehorst, T., O'Neill, P., Goodwin, P. M., Pennathur, S. & Fygenson, D. K. Distinct conformations of DNA-stabilized fluorescent silver nanoclusters revealed by electrophoretic mobility and diffusivity measurements. *Langmuir* **27,** 8923–8933 (2011).

15. Zuker, M. Mfold web server for nucleic acid folding and hybridization prediction. *Nucleic Acids Res.* **31,** 3406–3415 (2003).

16. Mathew-Fenn, R. S., Das, R. & Harbury, P. a B. Remeasuring the double helix. *Science* **322,** 446–449 (2008).

17. Triebel, H., Ineht, K. R. & Rassburger, J. Persistence length of DNA from hydrodynamic measurements. *Biopolymers* **10,** 2619–2621 (1971).

18. Chi, Q., Wang, G. & Jiang, J. The persistence length and length per base of single-stranded DNA obtained from fluorescence correlation spectroscopy measurements using mean field theory. *Phys. A Stat. Mech. its Appl.* **392,** 1072–1079 (2013).

19. Swasey, S. M., Leal, L. E., Lopez-Acevedo, O., Pavlovich, J. & Gwinn, E. G. Silver (I) as DNA glue: Ag+-mediated guanine pairing revealed by removing Watson-Crick constraints. *Sci. Rep.* **5,** 10163 (2015).

20. Förster, T. Transfer Mechanisms of Electronic Excitation. *Discuss. FARADAY Soc.* 7–17 (1959).

21. Griffin, J. *et al.* Size- and distance-dependent nanoparticle surface-energy transfer (NSET) method for selective sensing of hepatitis C virus RNA. *Chem. - A Eur. J.* **15,** 342–351 (2009).

22. Yun, C. S. *et al.* Nanometal Surface Energy Transfer in Optical Rulers, Breaking the FRET Barrier. *J. Am. Chem. Soc.* **127,** 3115–3119 (2005).

23. Ghosh, D. & Chattopadhyay, N. Gold and silver nanoparticles based superquenching of fluorescence: A review. *J. Lumin.* **160,** 223–232 (2015).

24. Darbha, G. K., Ray, A. & Ray, P. C. Gold Nanoparticle-Based Miniaturized Nanomaterial Surface Energy Transfer Probe for Rapid and Ultrasensitive Detection of Mercury in Soil, Water, and Fish. *ACS Nano* **1,** 208–214 (2007).

25. Conde, J., Rosa, J., de la Fuente, J. M. & Baptista, P. V. Gold-nanobeacons for simultaneous gene specific silencing and intracellular tracking of the silencing events. *Biomaterials* **34,** 2516–2523 (2013).

26. Singh, M. P., Jennings, T. L. & Strouse, G. F. Tracking Spatial Disorder in an Optical Ruler by Time-Resolved NSET. *J. Phys. Chem. B* **113,** 552–558 (2009).

27. Conde, J., Oliva, N. & Artzi, N. Implantable hydrogel embedded dark-gold nanoswitch as a theranostic probe to sense and overcome cancer multidrug resistance. *Proc. Natl. Acad. Sci.* **112,** E1278–E1287 (2015).

28. Jennings, T. L., Singh, M. P. & Strouse, G. F. Fluorescent Lifetime Quenching near d=1.5nm Gold Nanoparticles: Probing NSET Validity. *J. Am. Chem. Soc.* 5462–5467 (2006).

29. Gwinn, E., Schultz, D., Copp, S. M. & Swasey, S. DNA-Protected Silver Clusters for Nanophotonics. *Nanomaterials* **5,** 180–207 (2015).

30. O'Neill, P. R., Young, K., Schiffels, D. & Fygenson, D. K. Few-atom fluorescent silver clusters assemble at programmed sites on DNA nanotubes. *Nano Lett.* **12,** 5464–9 (2012).

31. Bossert, N., De Bruin, D., Götz, M., Bouwmeester, D. & Heinrich, D. Fluorescence-tunable Ag-DNA biosensor with tailored cytotoxicity for live-cell applications. *Sci. Rep.* **6,** (2016).

32. Guo, W., Yuan, J., Dong, Q. & Wang, E. Highly Sequence-Dependent Formation of Fluorescent Silver Nanoclusters in Hybridized DNA Duplexes for Single Nucleotide Mutation Identification. *J. Am. Chem. Soc.* **132,** 932–934 (2010).

33. Schultz, D. *et al.* Dual-color nanoscale assemblies of structurally stable, few-atom silver clusters, as reported by fluorescence resonance energy transfer. *ACS Nano* **7,** 9798–9807 (2013).